10.2478/v10170-010-0037-0

Archives of Control Sciences
Volume 21(LVII), 2011
No. 2, *pages 151–165*

Evaluation of maximum power point tracking methods for photovoltaic systems

ABDELAZIZ TALHA, HOURIA BOUMAARAF and OMAR BOUHALI

The output characteristics of photovoltaic (PV) arrays are nonlinear and change with the solar irradiance and the cell's temperature. Therefore, a maximum power point tracking (MPPT) technique is needed to draw peak power from the solar array to maximize the produced energy. Among the hill climbing methods, the perturb and observe (P&O) method tracks the maximum power point (MPP) by repeatedly increasing or decreasing the output voltage at the MPP of the PV module. The implementation of the method is relatively simple, but it cannot track the MPP when the irradiance varies quickly with time. In addition, it may cause system oscillation around the peak power points due to the effect of measurement noise. The incremental conductance (IncCond) method is also often used in PV systems. This method tracks the MPPs by comparing the incremental and instantaneous conductances of the solar array. This method requires longer conversion time, and a large amount of power loss results. In addition, extra hardware circuitry is required to implement the system. In this paper, it is shown that the negative effects associated with such a drawback can be greatly reduced if the intelligent method is used to improve P&O and IncCond algorithms. The perturbation step is continuously approximated by using fuzzy logic controller (FLC). By the digital simulation, the validity of the proposed control algorithm is proved.

Key words: maximum power point tracking, PV, P&O, incremental conductance, fuzzy logic, converter

1. Introduction

As the conventional energy sources are rapidly depleting, the importance of solar photovoltaic (PV) energy has been emerging as replaceable energy resources to human being. Since it is clean, pollution-free, and inexhaustible, researches on the PV power generation system have received much attention, particularly, on many terrestrial applications. Furthermore, due to the continuing decrease in PV arrays cost and the increase in their efficiency, PV power generation system could be one of comparable candidates as energy sources for mankind in the near future. As is well known, the output power of PV

A. Talha and H. Boumaaraf are with Laboratory of Instrumentation, Faculty of Electronics and Computer, University of Sciences and Technology Houari Boumediene, BP 32 El-Alia 16111 Bab-Ezzouar. Algiers, Algeria. Emails: abtalha@gmail.com, boumaaraf.houria@gmail.com. O. Bouhali is with LAMEL Laboratory, Jijel University, BP 98, Ouled Aissa, Jijel, Algeria. E-mail: bouhali_omar@yahoo.fr.

Received 12.04.2011.

cell is changed by environmental factors, such as irradiance and temperature [1]. Since the characteristic curve of the solar cell exhibits a nonlinear voltage-current characteristic, a controller named maximum power point tracker (MPPT) is required to match the solar cell power to the environmental changes. Many algorithms have been developed and implemented for tracking maximum power point of the solar cell [2][3]. The methods differ with respect to complexity, sensors required, convergence speed, cost, range of effectiveness, implementation hardware, popularity, and in other aspects. In this paper, we study three methods of search for MPP: P&O, IncCond and fuzzy logic. The perturbation and observation is one of the most commonly used MPPT methods for its simplicity and easiness of implementation [2][4]. The P&O works well when the irradiance change slowly but it presents drawbacks such as slow response speed, oscillation around the MPP in steady state, and even tracking in wrong way under rapidly changing atmospheric conditions [2][5]. For the second algorithm which is the IncCond we calculate the derivative of the exit power of the panel. This derivative vanishes at the point of maximum power, and becomes positive on the left and negative on the right side of the MPP point. This algorithm has the same problem that P&O. A numerical method based in fuzzy logic is proposed to solve this problem.

2. Description of the photovoltaic generator

Electrical equivalent circuit of the solar cell is shown in Fig. 1. It is composed of a light-generated current source, two diodes, series resistance, and parallel resistance.

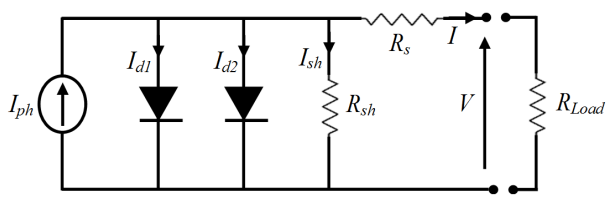

Figure 1. Equivalent electrical circuit for the PV cell.

Characteristic equation for the current and voltage of a solar cell is given by [6]:

$$I = I_{ph} - I_{s1}\left[\exp\left(\frac{q(V+R_sI)}{n_1kT}\right)-1\right] - I_{s2}\left[\exp\left(\frac{q(V+R_sI)}{n_2kT}\right)-1\right] - \frac{V+R_sI}{R_{sh}} \quad (1)$$

where I is the solar-cell output current (A), V is the solar cell output voltage (V), I_{ph} is the light generated current (A), I_{s1} and I_{s2} are the first and the second diode reverse saturation current respectively (A), q is the electronic charge (equal to $1.6\cdot10^{-19}$C, n_1 and n_2 are dimensionless deviation factor of the first and the second diode respectively, k is Boltzmann's constant $(1.3807\cdot10^{-23}$ JK$^{-1})$, T is the cell temperature (K), R_s is the series resistance (Ω), and R_{sh} is the shunt resistance (Ω). The equivalent circuit for the

solar cells arranged in n_p-parallel and n_s-series is shown in Fig. 2 and the mathematical equation relating the array current to the array voltage becomes [7] as follows:

$$\begin{aligned} I_G &= n_p I_{ph} - n_p I_{s1}\left[\exp\left(\frac{q(V_G + R_s I_G)}{n_s n_1 kT}\right) - 1\right] \\ &- n_p I_{s2}\left[\exp\left(\frac{q(V_G + R_s I_G)}{n_s n_2 kT}\right) - 1\right] - \frac{V_G + R_s I_G}{R_{sh}} \end{aligned} \tag{2}$$

where

$$I_{S1} = K_1 T^3 \exp\left(-\frac{E_g}{kT}\right), \tag{3}$$

$$I_{S2} = K_2 T^{5/2} \exp\left(-\frac{E_g}{kT}\right) \tag{4}$$

and: $K_1 = 1.2\text{A/cm}^2\text{K}^3$, $K_2 = 2.9\text{A/cm}^2\text{K}^{5/2}$, E_g is gap energy ($E_g = 1.12\text{eV}$), n_p represents the number of parallel modules. Note that each module is composed of n_s cells connected in series. $n_p I_{ph}$ corresponds to the short-circuit current of the solar array.

Placing the solar cells in series allows for heightening of the voltage, while placing the solar cells in parallel enables to reach what is needed by charging operation. Mixed this grouping would deliver a current $n_p I$ under the voltage $n_s V$ (I, V are the current and the voltage of the solar cell).

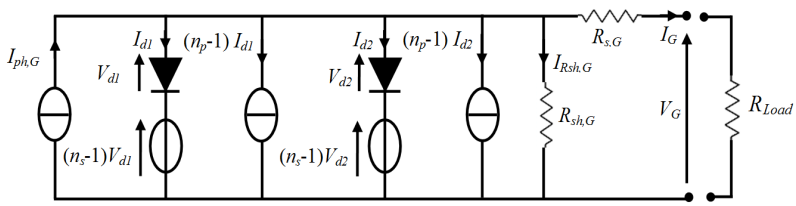

Figure 2. Equivalent electrical circuit for the PV panel.

3. Influence of meteorological parameters on the photovoltaic generator operating

The PV array characteristic presents three important elements: the short circuit current I_{sc}, the open circuit voltage V_{oc} and the optimum power P_{op} delivered by the PV array to an optimum load R_{op} when the PV modules operate at their MPP. Figures 3 and 4 present the current-voltage ($I-V$) and power-voltage ($P-V$) characteristics of the PV module for different values of solar radiation and temperature.

The short circuit current is clearly proportional to the solar radiation (Fig. 3): more radiation, more current, and also more maximum output power. On the other hand, the

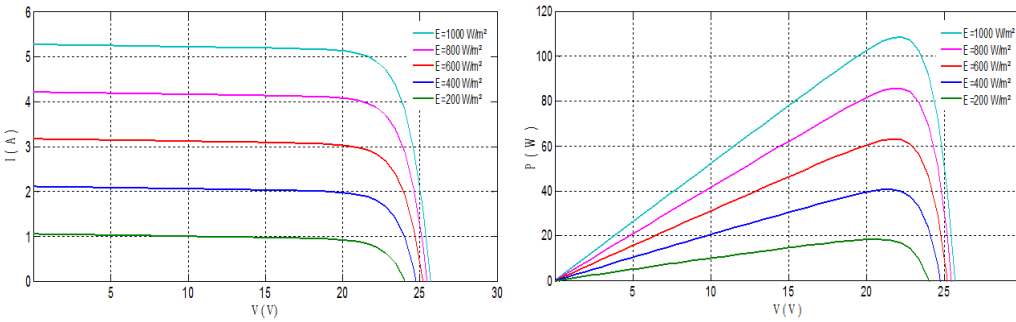

Figure 3. The effect of the irradiation on PV generator.

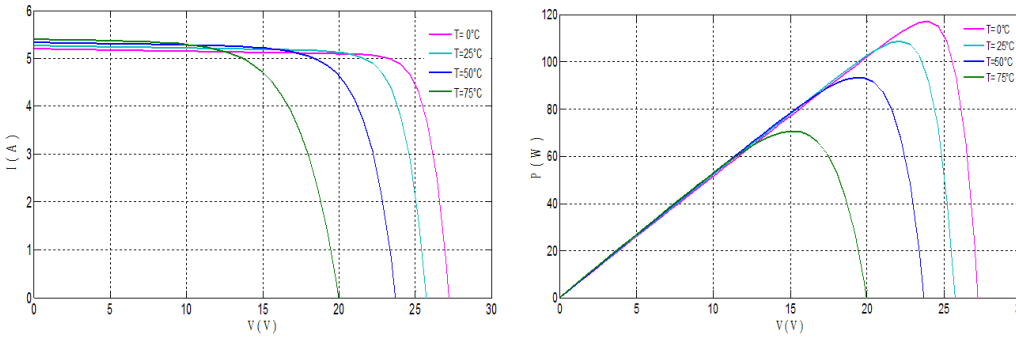

Figure 4. The effect of the cell temperature on PV generator.

temperature dependence is reversed (Fig. 4): an increase in temperature causes a reduction of the open-circuit voltage (when sufficiently high) and hence also of the maximum output power. These opposite effects of the variations of solar radiation and temperature on the maximum output power make them important if efficiency of tracking the MPP is concerned. The power curves in Fig. 3 and 4 show that the optimum power point corresponds to a load connected with the PV array that varies with the ambient conditions of illumination and temperature. In practice variable optimal load will be achieved through the use of a variable duty cycle of the control part of the MPPT converter, which controls directly the operating voltage which in turns corresponds to this optimal load.

4. MPPT converter

Figure 5 shows the MPPT buck-boost converter diagram. The converter is composed of a power part and a control part.

The switch *S* of the buck-boost converter is a MOSFET transistor with a low internal resistance R_{on}. The MOSFET is controlled by a PWM signal generation circuit that

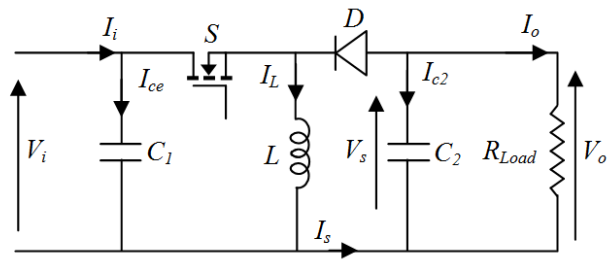

Figure 5. MPPT buck-boost converter.

uses a micro-controller. T is the period of the control signal and δ is the duty cycle. The switch S is closed for the time δT and opened for the time $(1-\delta)T$ during each period [6][8]. In searching for the MPP and tracking this point in order to minimize the spread between the operating power and the optimal power in the event of change of the meteorological conditions, the control circuit of the buck-boost converter artificially perturbs periodically the operating point of the PV module. The resulting output voltage and current of the PV modules are then used by the control circuit to increase or decrease the duty cycle of the buck-boost converter in order to change the operating point of the PV array. If the power is thereby increased, then the next perturbation will be in the same direction, otherwise the next perturbation will be in the opposite direction. The operation of the buck-boost converter is characterized as follows [9].

When the transistor S is closed, the current in the inductance L grows from I_m to I_M and the voltage across the inductance is given by:

$$V_L = V_i = L\frac{dI_L}{dt} = \frac{I_M - I_m}{t_{on}}L. \tag{5}$$

When the transistor is opened, the voltage is:

$$V_L = V_o = L\frac{dI_L}{dt} = \frac{I_M - I_m}{t_{off}}L. \tag{6}$$

From equations (5) and (6) we get:

$$(I_M - I_m)L = V_i t_{on} = V_o t_{off}. \tag{7}$$

The average output voltages are determined by the following equation:

$$M(\delta) = \frac{V_o}{V_i} = \frac{1}{1+\frac{R_L I_0}{(1-D)^2 V_0}}\frac{-\delta}{1-\delta} \tag{8}$$

where V_o and V_i are the output and input voltage of the converter and D is the perturbation step size of the switch S.

5. Different algorithms MPPT

As is well known, the MPP of PV power generation system depends on array temperature and solar irradiation, so it is necessary to constantly track MPP of solar array. For years, research has focused on various MPP control algorithms to draw the maximum power of the solar array. In this section, the effectiveness of three different control algorithm are thoroughly investigated via numerical simulation.

5.1. Perturbation and observation algorithm

Perturbation and observation method has been often used because it is easy to implement. P&O algorithm forces the PV system to approach to the maximum power point by increasing or decreasing the PV panel output voltage [10]. To adapt the PV panel voltage a DC/DC converter is inserted between the solar panel and the load. The variation of the PV panel voltage is achieved by varying the converter duty cycle.

As its name indicates, P&O method performs disturbances of V_{pv} and the observation of its impact on the change of the exit power of panel statement [11] [12]. Figure 6 presents the control flow chart of the P&O algorithm.

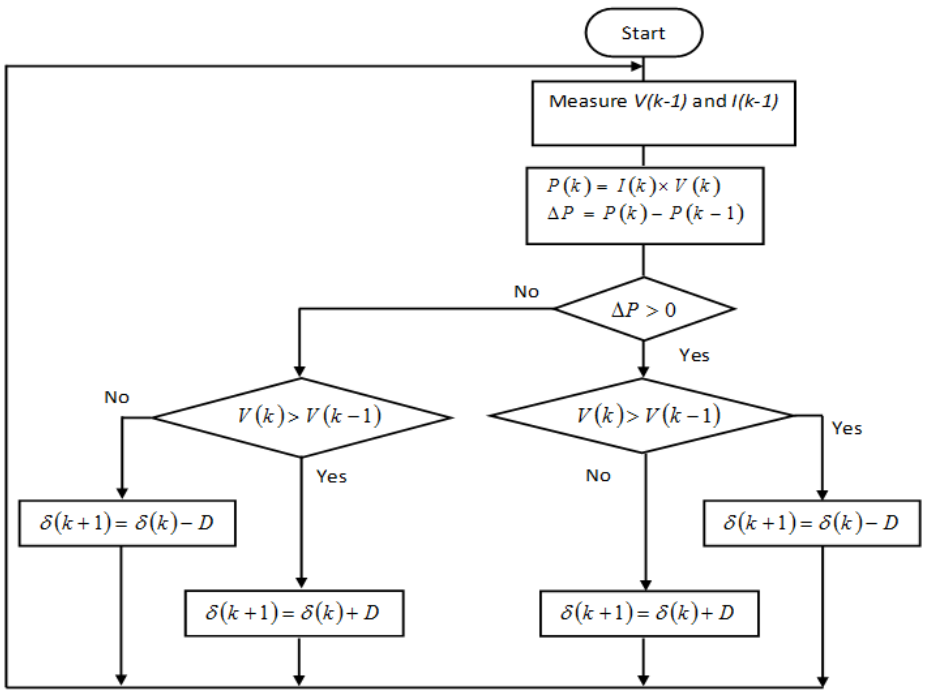

Figure 6. Flowchart of the P&O algorithm .

In order to find the direction change for maximizing power, the P&O method perturbs the operating voltage of the PV panel. If the power of exit increases compared to the previous measurement, the disturbance of the output voltage (V_{PV}) is continued in the same direction that was taken with the last cycle. If the power of exit decreased compared to the previous measurement, V_{PV} is disturbed in the opposite direction then in the last iteration. V_{PV} is thus disturbed with each cycle of MPPT. When the point of maximum power is reached, V_{PV} oscillates around optimal value V_{OP}.

Duty cycle perturbation at time $(t+1)$ can be determined on the basis of the following relationship [11]:

$$\delta(t+1) = \delta(t) + (2 \cdot \text{Sign} - 1)D \tag{9}$$

where Sign is given by:

$$\text{Sign} = ([P(t) - P(t-1)] > 0) \oplus ([V(t) - V(t-1)] > 0), \tag{10}$$

$P(t)$ and $V(t)$ are, respectively, power and voltage drawn from the PV panel.

Figure 7 shows the effect of the perturbation step size D of the converter on the evolution of the operating point of the photovoltaic generator.

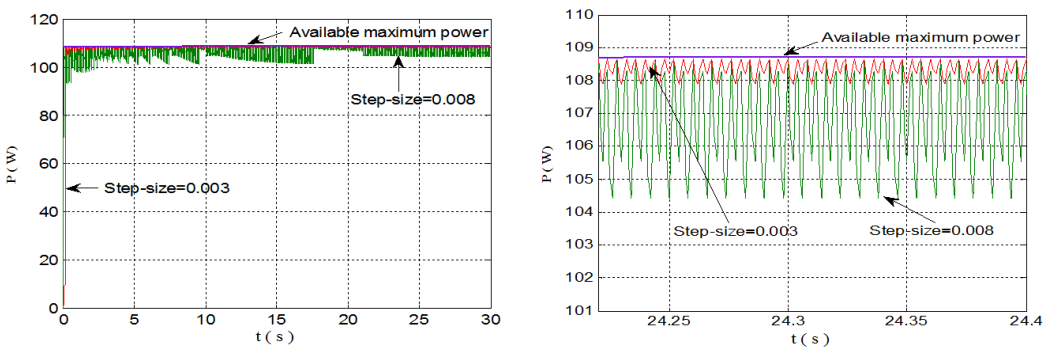

Figure 7. Perturbation step-size effects on the performances of the P&O algorithm.

Amplitude of the command oscillation depends directly on the perturbation step size constant of the converter. The oscillation around the MPP can be minimized by reducing the perturbation step size D. However, dynamic performance is hampered by smaller perturbation step size. This trade off requires careful tuning of the duty cycle perturbation step size.

5.2. Incremental conductance algorithm

The incremental conductance method is based on the fact that the slope of the PV array power curve is zero at the MPP, positive on the left of the MPP, and negative on

the right, as given in [12]:

$$\begin{cases} \frac{\Delta I}{\Delta V} + \frac{I}{V} = 0 & \text{at PPM} \\ \frac{\Delta I}{\Delta V} + \frac{I}{V} > 0 & \text{left of PPM} \\ \frac{\Delta I}{\Delta V} + \frac{I}{V} < 0 & \text{right of PPM.} \end{cases} \tag{11}$$

Because of the noise, measurement's faults and the quantification, the condition $(\Delta I/\Delta V) + (I/V) = 0$ is seldom satisfied, therefore in steady state, the system oscillate around the MPP. To overcome this drawback we introduce a new parameter ε, as:

$$\left| \frac{\Delta I}{\Delta V} + \frac{I}{V} \right| \leqslant \varepsilon. \tag{12}$$

The value of the parameter ε is to be chosen carefully for improved performance of the MPPT system.

The incremental conductance algorithm is shown in form of the flowchart in Fig. 8 [12].

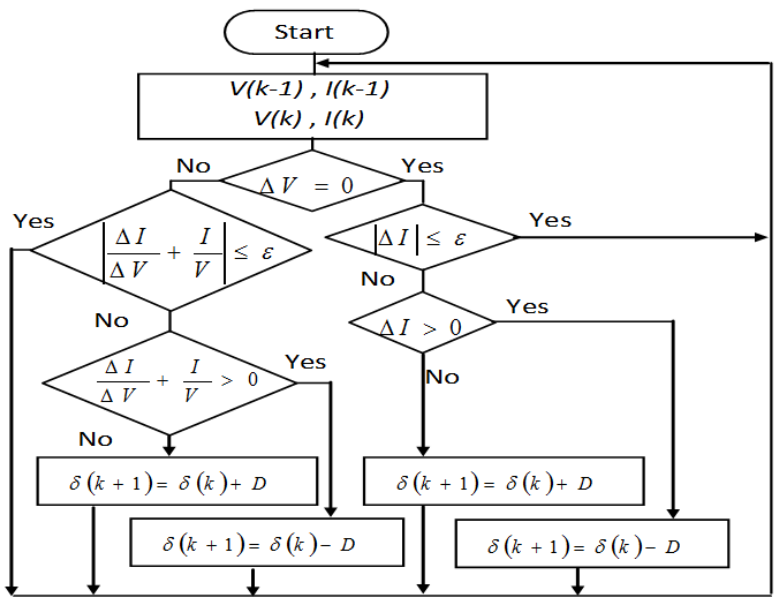

Figure 8. Flowchart of the incremental conductance algorithm.

Figure 9 shows the effect of the abruptly change in metrological parameters on the evolution of the operating point of the photovoltaic generator.

It is noticed that if the solar irradiation increases abruptly, incremental conductance algorithm loses the point of maximum power. The point of operation deviates on the left or on the right side of its optimal value. When the value of the irradiation is stabilized,

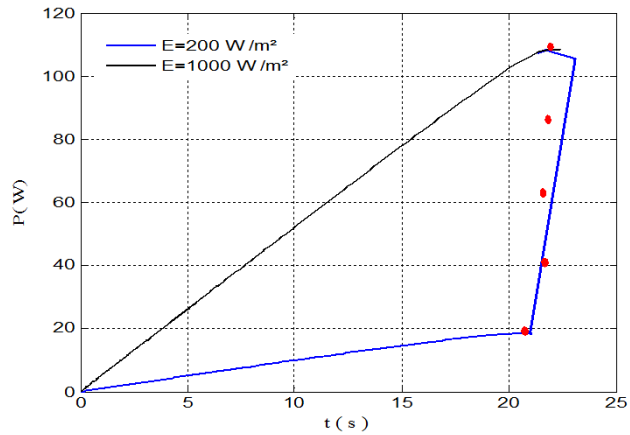

Figure 9. Incremental conductance operating point path.

the algorithm takes again control and the point of operation converges quickly towards its optimal position.

5.3. Fuzzy logic controller algorithm

Fuzzy logic controllers have the advantages of working with imprecise inputs, not needing an accurate mathematical model, and handling nonlinearity [2]. Fuzzy logic control generally consists of three stages: fuzzification, rule base table lookup, and defuzzification. The inputs of the fuzzy logic controllers are an error E and an error variation CE, the output is a duty cycle or its variation. The user can flexibly choose the way of computing E and CE [12][13].

$$\begin{cases} E(k) = \frac{P(k)-P(k-1)}{V(k)-V(k-1)} \\ CE(k) = E(k) - E(k-1). \end{cases} \tag{13}$$

During fuzzification, numerical input variables are converted into linguistic variables based on a membership function as shown in Fig. 10. In this case, five fuzzy levels are used: NB (Negative Big), NS (Negative Small), ZE (Zero), PS (Positive Small), and PB (Positive Big). The membership function is sometimes composed asymmetrically to provide different importance to specific fuzzy levels [14] [15].

The kernel of fuzzy logic controller is the fuzzy inference system. Fuzzy inference is the process of formulating the mapping from a given input to the output using fuzzy logic. The mapping then provides a basis from which decisions can be made (see Fig. 11). The proposed Mamdani-type inference system endeavours to force the error function to zero. Two cases are to consider:

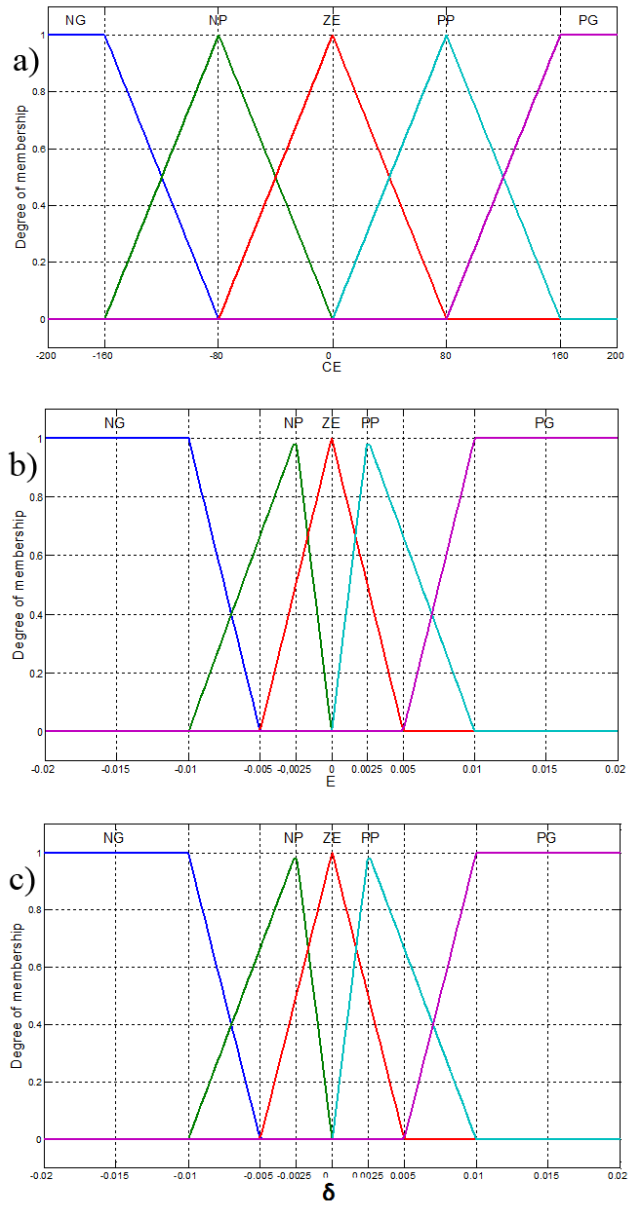

Figure 10. Membership function.

- **First case**: *E* is positive; working point is on the left side of the MPP. If the change of error *CE* is positive, then the working point converges toward the MPP. If *CE* is negative, then reverse action occurs.

		CE				
		NG	NP	ZE	PP	PG
E	NG	ZE	ZE	PG	PG	PG
	NP	ZE	ZE	PP	PP	PP
	ZE	PP	ZE	ZE	ZE	NP
	PP	NP	NP	NP	ZE	ZE
	PG	NG	NG	NG	ZE	ZE

Group 1
Group 2
Group 3
Group 4

Figure 11. Inference matrix.

- **Second case**: E is negative; working point is, therefore, on the right side of the MPP. In this case if CE is positive, working point moves away of the MPP and vice versa if CE is negative.

Finally, in the defuzzification stage, the fuzzy logic controller output is converted from a linguistic variable to a numerical variable. This provides an analog signal that will control the power converter to the MPP.

6. Simulation results

Three studied MPPT algorithms are compared in terms of tracking capability at steady state (Fig. 12) and variable environmental conditions (Fig. 13, 14, 15 and 16). At standard conditions ($E = 1000\text{W/m}^2$ and $T = 25^o\text{C}$).

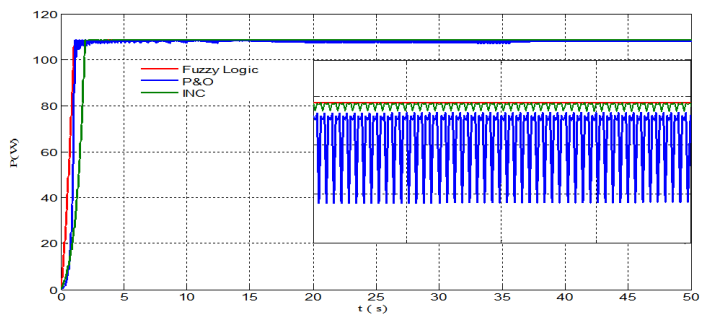

Figure 12. Comparing controllers performances in a standards atmospherics conditions.

It is noticed that the undulations of P&O around PPM are much greater than in the case of incremental conductance algorithm and fuzzy logic. The last one follows the PPM very well and thus it remains the best method among the three algorithms studied.

Under a constant temperature, we increased the irradiance between 600W/m^2 and 1000W/m^2 during 20s, and after 10s of stabilization we decreased the irradiance with the same value during 20s as well. This experiment showed effect of irradiance variation.

We studied also the effect of temperature variation on the evolution of the operating point of the photovoltaic panel. For a standard irradiance (E=1000W/m^2), we increased the temperature between 25^{o}C and 75^{o}C during 30s, and after 20s of stabilization we decreased the temperature with the same value during another 30s.

Figures 13, 14, 15 and 16 show the transient responses of the tracked power obtained from the three MPP controllers.

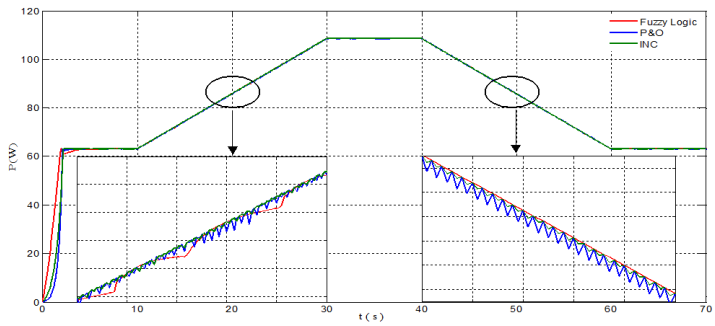

Figure 13. Comparison of powers under variable atmospheric conditions, T=25^{o}C.

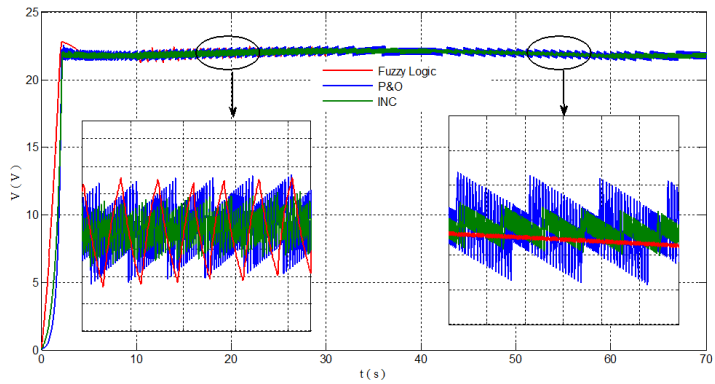

Figure 14. Comparison of voltages under variable atmospheric conditions, T=25^{o}C.

It can be observed that the FLC reaches MPP faster compared to the other controllers. Steady state behavior of the PV system using FLC is more stable than the other MPPT methods. Power's waste is here considerably reduced.

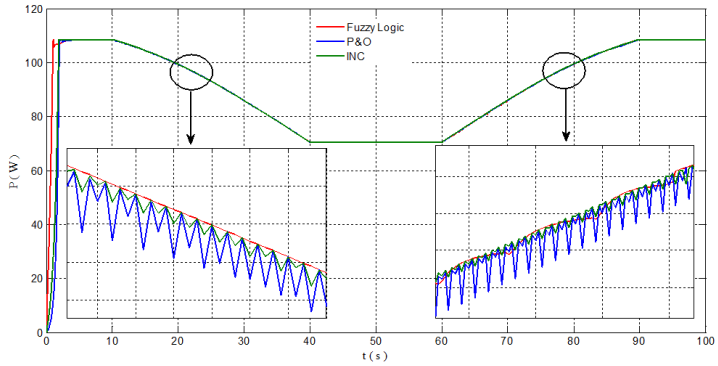

Figure 15. Comparison of powers under variable atmospheric conditions, E=1000W/m^2.

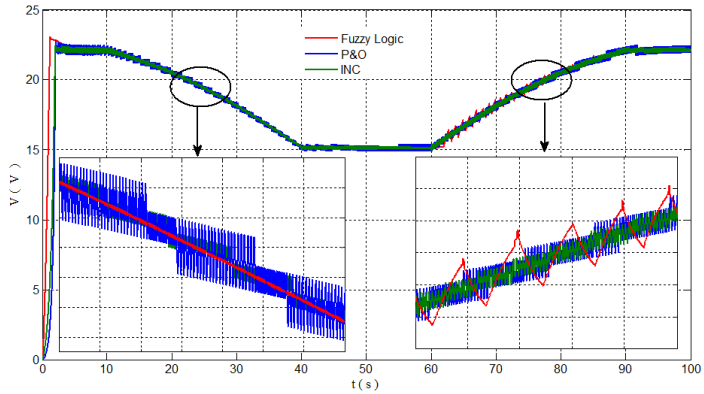

Figure 16. Comparison of voltages under variable atmospheric conditions, E=1000W/m^2.

7. Conclusion

In this paper we studied three topologies of MPPT, each one with its advantages and disadvantages. The choice depends on the applications for which they are intended.

Perturb and observe and incremental inductance controllers are very simple to implement and can be carried out easily. Drawbacks of these algorithms occur at steady state where the system's operating point oscillates around the MPP giving rise loss of available power. Choosing of the perturbation step size is very critical. The step size determines how fast the MPP can be reached, fast tracking can be achieved with bigger step size, but the oscillations around the MPP occur. There is tradeoff between the dynamic and steady performance. The simulation results show that the use of fuzzy logic controller can improve the efficiency of the overall system by minimizing the energy losses when the change of irradiation is frequent when compare with the P&O and InC methods.

References

[1] K.H. HUSSEIN et al: Maximum photovoltaic power tracking: An algorithm for rapidly changing atmospheric conditions. *Proc. Inst. Elect. Eng.*, **142**(1), (1995), 59-64.

[2] T. ESRAM and P.L. CHAPMAN: Comparison of photovoltaic array maximum power point tracking techniques.*IEEE Trans. on Energy Conversion*, **22**(2), (2007), 439-449.

[3] M. VEERACHARY, T. SENJYU and K. UEZATO: Voltage-based maximum power point tracking control of PV system. *IEEE Trans. Aerosp. Electron. Syst.*, **38**(1), (2002), 262-270.

[4] T. TAFTICHT, K. AGBOSSOU, M.L. DOUMBIA and A. CHÉRITI: An improved maximum power point tracking method for photovoltaic systems. *Renewable Energy*, **33**(7), (2008), 1508-1516.

[5] J.A. DUFFIE and W.A. BECKMAN: Solar engineering of thermal process. John Wiley & Sons Ltd., 1980, 768-793.

[6] R. AKKAYA, A.A. KULAKSIZ and O. AYDOGDU: DSP implementation of a PV system with GA-MLP-NN based MPPT controller supplying BLDC motor drive. *Energy Conversion and Management*, **48** (2007), 210-218.

[7] S. ALEPUZ et al: Interfacing renewable energy sources to the utility grid using a three-level inverter. *IEEE Trans. on Industrial Electronics*, **53**(5), (2006), 1504-1511.

[8] G. SARAVANA ILANGO, P. SRINIVASA RAO, A. KARTHIKEYAN and C. NAGAMANI: Single-stage sine-wave inverter for an autonomous operation of solar photovoltaic energy conversion system. *Renewable Energy*, **35** (2010), 275-282.

[9] J.M. ENRIQUE, E. DURÀN, M. SIDRACH-DE-CARDONA and J.M. ANDÙJAR: Theoretical assessment of the maximum power point tracking efficiency of photovoltaic facilities with different converter topologies. *Solar Energy*, **81** (2007), 31-38.

[10] N. FEMIA, G. PETRONE, G. SPAGNOLO and M. VITELLI: Optimization of perturb and observe maximum power point tracking method. *IEEE Trans. on Power Electronics*, **20**(4), (2005), 963-973.

[11] N. FEMIA, G. PETRONE, G. SPAGNOLO and M. VITELLI: Increasing the efficiency of P&O by converter dynamic matching. *Proc. of 35th Annual IEEE Power Specialists Conf.*, Aachen, Germany, (2004).

[12] J. YOUNGSEOK, S. JUNGHUN, Y. GWONJONG and C. JAEHO: Improved perturbation and observation method (IP&O) of MPPT control for photovoltaic power systems. *Proc. of 31st Photovoltaic Specialists Conf.*, Lake Buena Vista, Florida, (2005), 1788-1791.

[13] T. WU, C. CHANG and Y. CHEN: A fuzzy-logic-controlled single-stage converter for PV-powered lighting system applications. *IEEE Trans. Ind. Electron.*, **47**(2), (2000), 287-296.

[14] R.M. HILLOOWALA and A.M. SHARAF: A rule-based fuzzy logic controller for a PWM inverter in photovoltaic energy conversion scheme. *Proc. IEEE Ind. Appl. Soc. Annu. Meet.*, (1992), 762-769.

[15] S. LALOUNIA, D. REKIOUA, T. REKIOUA and E. MATAGNE: Fuzzy logic control of stand-alone photovoltaic system with battery storage. *J. of Power Sources*, **193** (2009), 899-907.